Characteristics of Polystyrene/Organoclay Nanocomposites Prepared by In-Situ Polymerization with Macroazoinitiator Containing Poly(dimethylsiloxane) Segment

Han Mo Jeong, Ji Suk Choi, Young Tae Ahn, Kun Ho Kwon

Department of Chemistry and Research Center for Machine Parts and Materials Processing, University of Ulsan, Ulsan 680–749, Republic of Korea

Received 28 November 2004; accepted 15 April 2005
DOI 10.1002/app.22985
Published online in Wiley InterScience (www.interscience.wiley.com).

ABSTRACT: Polystyrene (PS)/organoclay nanocomposites were prepared by the *in situ* polymerization of styrene in the presence of organoclay with macroazoinitiator (MAI), composed of repeated sequences of poly(dimethylsiloxane) (PDMS) and azo groups. The X-ray diffraction patterns and the morphology observed with a transmission electron microscope showed that the dispersion of organoclay in polymer matrix improved as the content of the PDMS segment in the nanocomposite increased. However, negative effects on the rise of glass transition temperatures and the thermal resistance of nanocomposite, measured by differential scanning calorimetry and thermogravimetry, at a high content of the PDMS segment, suggested that organoclay lay preferentially in the PDMS domain. © 2005 Wiley Periodicals, Inc. J Appl Polym Sci 99: 2841–2847, 2006

Key words: polystyrene; organoclay; nanocomposites; macroazoinitiator; morphology

INTRODUCTION

Polymer/layered silicate nanocomposites exhibit markedly improved properties, when compared with pure polymers or conventional composites, because their unique intercalated or exfoliated structures maximize interfacial contact between the organic polymer and layered silicate, such as montmorillonite (MMT), which is composed of stacks of parallel lamellae with a 1 nm thickness and a high aspect ratio.[1–3]

The hydrophilic nature of a pristine MMT surface and a strong electrostatic interaction between silicate layers through intergallery cations impede the diffusion of a hydrophobic polymer chain into the gallery between silicate layers to make a nanocomposite. This difficulty can be overcome when interlayer cations, such as Na^+, Ca^+, or K^+, are replaced with organic cations, ammonium ions with long alkyl chains.[4–8] This organoclay has a low surface polarity and enhanced affinity with hydrophobic matrix polymers to make nanocomposites.

Polystyrene (PS)/organoclay nanocomposites have been reported to have mainly an intercalated structure.[4,5,9–11] Many researchers have tried to enhance the interaction between the PS chains and silicate surfaces of organoclay.[12–15] Doh and Cho reported that a structural affinity between the styrene monomer and the organic cation of organoclay played an important role in PS/organoclay nanocomposites.[16] Some researchers have also reported that polar comonomers, such as acrylonitrile, methylvinyl oxazoline, or maleic anhydride, enhanced the interaction between styrenic polymers and organoclay.[17,18] Efforts have also been made with reactive organoclays, which were modified with ammonium ions presenting polymerizable groups, to ensure the adherence of PS chains to silicate layers.[5,19,20]

Poly(dimethylsiloxane) (PDMS) has an affinity with organoclay for making an exfoliated nanocomposite.[21] Ishida et al., used PDMS as a swelling agent to enhance the diffusion of polymer chains into a gallery of organoclay.[4] So, we can assume that the compatibility of PS with organoclay will be improved by a PDMS block linked to PS, similar to the compatibility of hydrophobic polymers, such as PS, polyethylene, poly(methyl methacrylate) (PMMA), with hydrophilic sodium MMT being enhanced by hydrophilic poly(ethylene oxide) blocks linked to the polymers.[22,23]

The macroazoinitiator (MAI), composed of repeated sequences of PDMS and azo groups, can be effectively used for the radical polymerization of vinyl monomers to form PDMS–polyvinyl multiblock copolymers.[24–26] So in this study, to observe the effects of PDMS blocks linked to PS, MAI was used as a radical initiator to make a PS/organoclay nanocomposite by

Correspondence to: H. M. Jeong (hmjeong@mail.ulsan.ac.kr).
Contract grant sponsor: Research Center for Machine Parts and Materials Processing, Korea Science and Engineering Foundation.

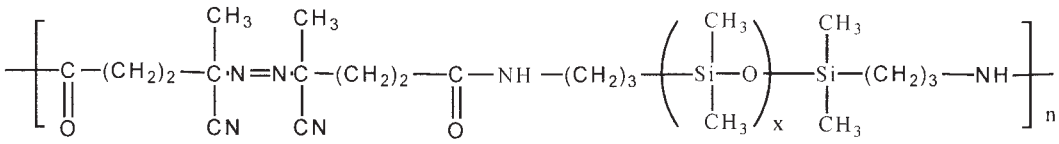

Scheme 1

in situ polymerization. The effect of the PDMS block on the structure and thermal properties of the nanocomposite was then examined.

EXPERIMENTAL

Materials

Organoclays, Cloisite 10A (C10A) and Cloisite 15A (C15A), were obtained from Southern Clay Products Inc. and dried for 2 h at 80°C under vacuum before use. C10A is a natural MMT modified with dimethyl benzyl hydrogenated tallow quaternary ammonium ion. The modifier concentration is 125 meq/100 g clay and the weight loss on ignition is 39%. The modifier of C15A is dimethyl dihydrogenated tallow quaternary ammonium ion. The modifier concentration and the weight loss on ignition of C15A are 125 meq/100 g clay and 43%, respectively. The MAI (Wako Pure Chemical, VPS-0501) with the chemical structure (as seen in Scheme 1)[26] was used as received. It is the condensation polymer of 4,4′-azobis(4-cyanovaleric acid) and α,ω-bis(3-aminopropyl) PDMS. The molecular weight of α,ω-bis(3-aminopropyl) PDMS is 5000 g/mol. The molecular weight of MAI is 30,000–50,000 g/mol and the azo group content is 0.2 mmol/g.[26] Styrene was washed with 0.1*M* aqueous sodium hydroxide solution and pure water. It was distilled under vacuum before polymerization after drying over anhydrous sodium sulfate. 2,2′-Azobisisobutyronitrile (AIBN, Aldrich) and *n*-hexane(Aldrich) were used as received.

Preparation of nanocomposites

To intercalate MAI between the galleries of organoclay, 1.25 g of MAI was dissolved in 10 mL of *n*-hexane and the solution was stirred with organoclay for 12 h. Organoclay treated with MAI was obtained by the evaporation of *n*-hexane under vacuum at 25°C. This organoclay treated with MAI was used to prepare PS/organoclay nanocomposite by *in situ* polymerization of styrene at 60°C under N_2 atmosphere for 48 h,

TABLE I
Recipe for the Preparation of PS/Organoclay Nanocomposite

	Feed					
				Organoclay		
Designation code	Styrene (g)	AIBN (g)	MAI (g)	C10A (g)	C15A (g)	Concentration of azo group (mmol/100 g styrene)
Series I						
C00S0	99.661	0.339	—	—	—	2.041
C00S1	95.247	—	4.753	—	—	0.998
C00S2	90.990	—	9.010	—	—	1.980
C00S3	83.333	—	16.667	—	—	4.000
C00S4	76.923	—	23.077	—	—	6.000
C00S5	67.480	—	35.520	—	—	10.528
Series II						
C10S0	94.966	0.286	—	4.748	—	1.807
C10S1	90.909	—	4.545	4.545	—	1.000
C10S2	87.146	—	8.497	4.357	—	1.950
C10S3	80.274	—	15.902	3.824	—	3.962
C10S4	73.725	—	22.589	3.686	—	6.128
C10S5	64.267	—	32.455	3.278	—	10.100
Series III						
C15S0	94.966	0.286	—	—	4.748	1.807
C15S1	90.810	—	4.613	—	4.577	1.016
C15S2	86.813	—	8.803	—	4.384	2.208
C15S3	79.891	—	16.082	—	4.027	4.026
C15S4	74.019	—	22.235	—	3.745	6.008
C15S5	64.483	—	32.241	—	3.276	10.000

TABLE II
Molecular Weight of Matrix Polymer and Polymerization Yield

Sample	Molecular weight (g/mol) $\bar{M}_n$	Molecular weight (g/mol) $\bar{M}_w$	Polymerization yield (%)
Series I			
C00S0	103,000	509,000	93.9
C00S1	251,000	3,761,000	80.8
C00S2	144,000	2,275,000	83.5
C00S3	176,000	3,081,000	87.2
C00S4	187,000	3,816,000	85.7
C00S5	166,000	3,327,000	84.6
Series II			
C10S0	134,000	627,000	61.7
C10S1	131,000	1,451,000	55.1
C10S2	—	—	61.0
C10S3	199,000	2,409,000	73.0
C10S4	—	—	78.0
C10S5	210,000	1,463,000	82.0
Series III			
C15S0	101,000	255,000	59.8
C15S1	210,000	1,874,000	63.4
C15S2	239,000	3,606,000	63.4
C15S3	213,000	3,175,000	74.6
C15S4	168,000	2,445,000	81.4
C15S5	174,000	3,795,000	84.9

with stirring by a magnetic bar. The prepared PS/organoclay nanocomposites were crushed into powder and dried at 80°C for 24 h under vacuum to remove low molecular weight components. The recipes for the preparation of the PS/organoclay nanocomposite are shown in Table I, where Series I is reference samples containing no organoclay, and Series II and Series III are the nanocomposites of C10A and C15A, respectively.

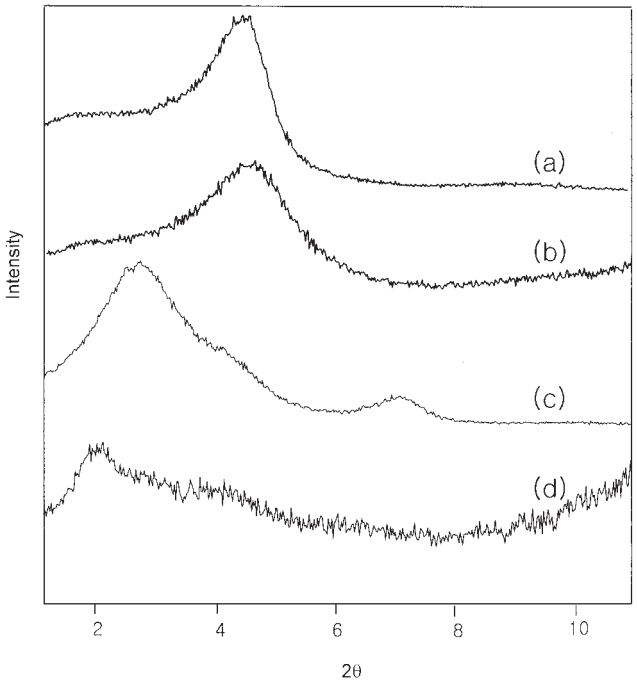

Figure 1 XRD patterns of (a) C10A, (b) C10A/MAI (33.9/66.1 by weight), (c) C15A, and (d) C15A/MAI (33.2/66.8 by weight).

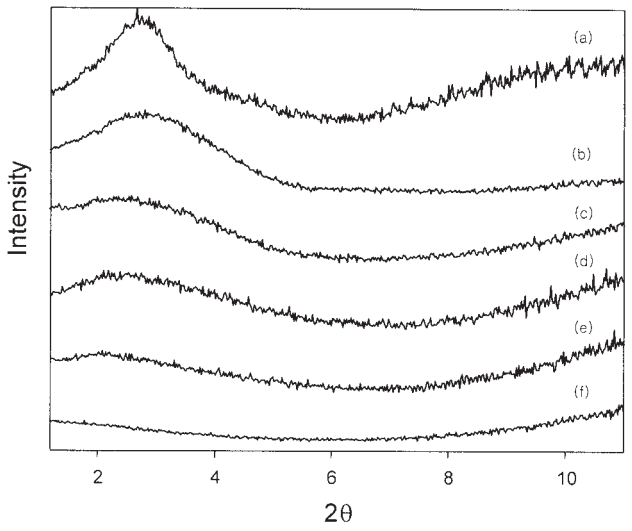

Figure 2 XRD patterns of PS/C10A nanocomposites: (a) C10S0, (b) C10S1, (c) C10S2, (d) C10S3, (e) C10S4, and (f) C10S5.

Measurements

Number–average molecular weight ($\bar{M}_n$) and weight–average molecular weight ($\bar{M}_w$) were evaluated at 43°C with gel permeation chromatography (GPC, Waters M510). Tetrahydrofuran was used as an eluant.

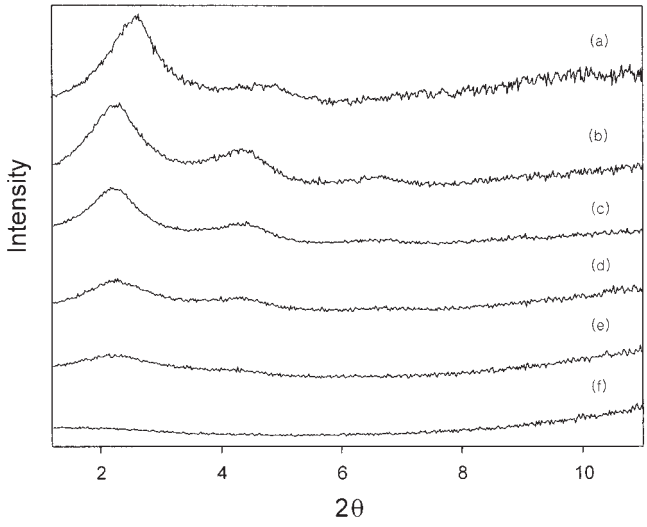

Figure 3 XRD patterns of PS/C15A nanocomposites: (a) C15S0, (b) C15S1, (c) C15S2, (d) C15S3, (e) C15S4, and (f) C15S5.

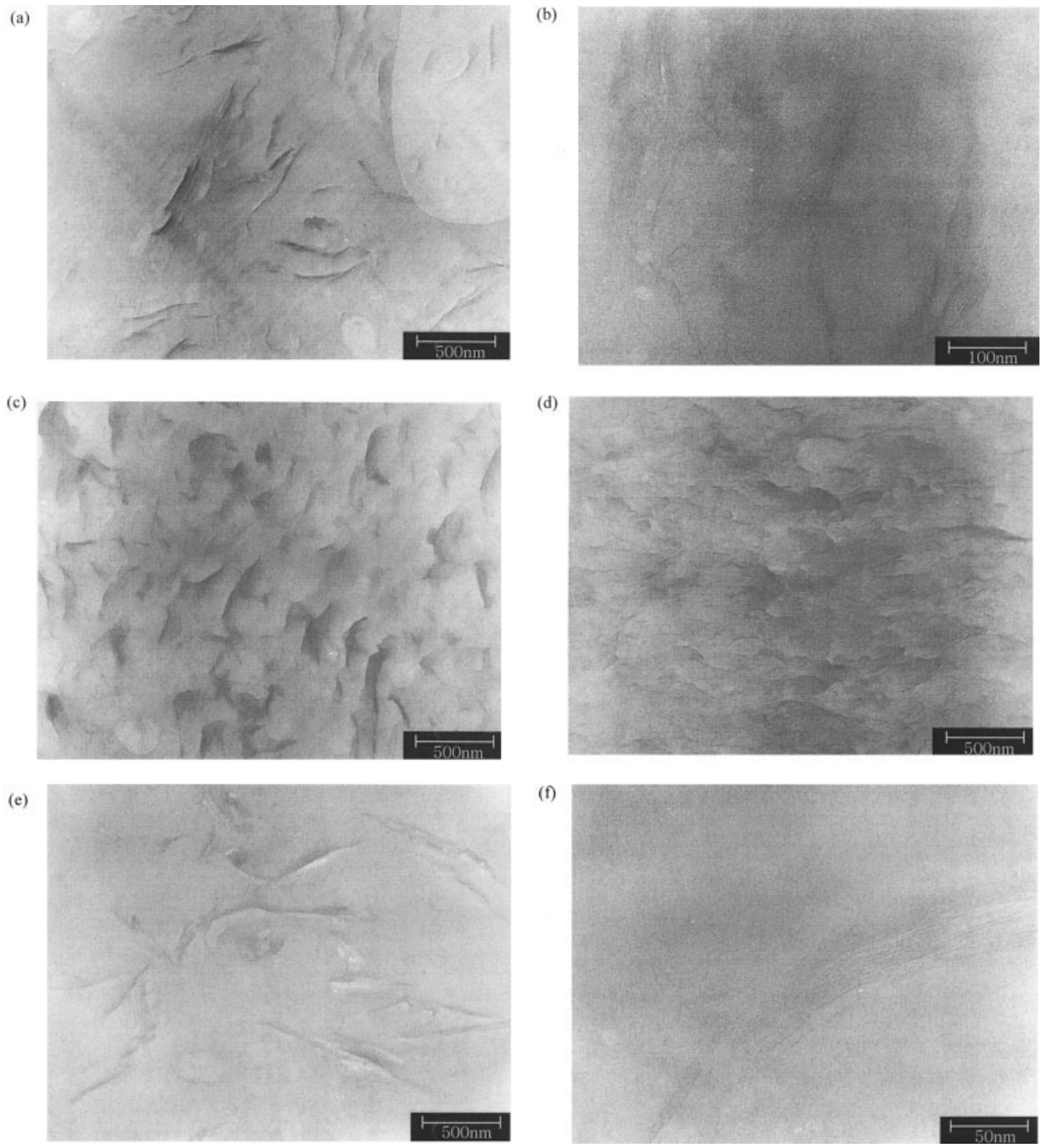

Figure 4 TEM images: (a) and (b) C10S0, (c) C10S2, (d) C10S5, (e) and (f) C15S0, (g) and (h) C15S2.

X-ray diffraction (XRD) patterns were obtained with an X-ray diffractometer (X'PERT, Philips) using CuKα radiation ($\lambda = 1.54$ Å) as the X-ray source. The diffraction angle was scanned from 1.2° at a rate of 1.2°/min.

The morphology of the nanocomposites was examined with a transmission electron microscope (TEM, Hitachi H-8100) with an accelerating voltage of 200 kV. The samples for TEM observation were first prepared by putting a nanocomposite into an epoxy capsule and curing the epoxy at 25°C for 24 h in a vacuum oven. Then, the cured epoxy containing a nanocomposite was microtomed by a diamond knife into 80-nm thick slices.

Differential scanning calorimetry (DSC) was carried out with a DSC-2910 (TA Instrument) at a heating and cooling rate of 10°C/min, with 5 mg of sample. The sample stayed at 150°C for 5 min in the DSC, and was then cooled down to 25°C. The glass transition temperature (T_g) was determined in a subsequent heating scan.

Thermogravimetric analysis (TGA) was carried out with a thermogravimetric analyzer (TA Instruments,

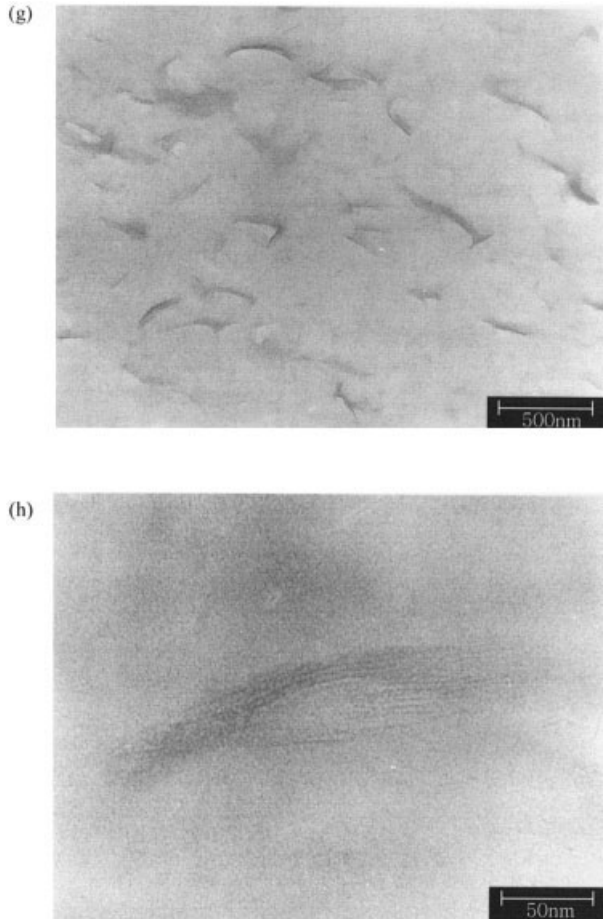

Figure 4 (*Continued from previous page***)**

TGA-2950) at a heating rate of 10°C/min under N_2 atmosphere, with a sample of 5 mg in a platinum crucible.

RESULTS AND DISCUSSION

Polymerization

The molecular weight of matrix polymers, analyzed by GPC, and polymerization yield are shown in Table II. The matrix polymers polymerized with MAI have much higher molecular weight than those polymerized with AIBN. This shows that termination by the coupling reaction can yield a large multiblock copolymer of PS and PDMS blocks, because an MAI molecule has many azo groups linked by PDMS blocks.[24]

Table II also shows that polymerization yields of Series II and III decrease in the presence of organoclay, when the initiator concentration is low, compared with Series I. This suggests that some initiators are intercalated in the gallery between silicate layers, and a strong case effect, which reduces the initiator efficiency, exists when the azo groups were thermally dissociated in this narrow gallery.[27] Clays are known to be free-radical scavengers and traps, because the clay minerals inhibit the free radical reactions by absorption of the propagating or initiating radicals to the Lewis acid surface. This may be another cause of yield reduction in the presence of clay.[6]

XRD

Figure 1 shows the XRD patterns of C10A and C10A treated with MAI in *n*-hexane. C10A had an XRD peak of $2\theta = 4.6°$.[16] This peak position suggests that a lateral bilayer arrangement of long alkyl chain is preferred in the gallery.[28] This peak position did not evidently vary when treated with MAI in *n*-hexane for intercalation, as described in the experimental section. This suggests that MAI molecules were not intercalated between the galleries of C10A. Figure 1 shows that C15A had an XRD peak of $2\theta = 2.8°$.[16] This peak position suggests that paraffin-type arrangement of long alkyl chain is preferred in the gallery because of high packing density of long alkyl chain in the gallery.[28] This peak position moved to $2\theta = 2.2°$ with reduced intensity by the treatment with MAI in *n*-hexane for intercalation. This shift of peak to a lower angle shows that the gallery height calculated by Bragg's law, $d = \lambda/2 \sin \theta$, was increased from 31.5 to 40.1 Å by the intercalation of MAI molecules, and that a reduction of the peak intensity suggested that some of the ordered parallel face–face morphology of silicate layers were disordered. These results are similar to those reported by Burnside and Giannelis.[21] They observed that C15A delaminated in the PDMS matrix when sonicated at room temperature; however, organoclay modified with benzyl dimethyl octadecyl ammonium ion was neither intercalated nor delaminated. The above results indicate that modifiers with benzyl groups as in C10A are not properly matched for the dispersion of organoclay in a PDMS matrix.

Figure 2 shows the XRD patterns of PS/C10A nanocomposites. C10S0, which was polymerized with AIBN, had a peak at $2\theta = 2.7°$, being at a lower angle when compared to that of C10A at $2\theta = 4.6°$ [Fig. 1(a)]. This shows that the gallery height was increased from 19.2 to 32.7 Å by the intercalated PS molecules.[9,16] However, this peak moved further to a lower angle and became obscure as the amount of MAI used for polymerization was increased. That is, C10S2, which was prepared at an azo group concentration similar to that of C10S0, had a broad peak around $2\theta = 2.2°$, and the peak became featureless in the XRD patterns of C10S4 and C10S5. This change of XRD pattern shows that a disordering of the intercalated structures of C10A was enhanced by the PDMS segment linked to a PS chain. In Figure 3, C15S0, which was polymerized with AIBN, has a peak at $2\theta = 2.5°$, at a slightly lower angle compared to that of C15A at $2\theta = 2.8°$ [Fig. 1(c)], showing a minute increase of gallery height from 31.5 to 35.3 Å. These results suggest that although C15A

TABLE III
Thermal Properties of PS/Organoclay Nanocomposite

Sample	Glass transition temperature (°C)		20% weight loss temperature (°C)	
	T_g	ΔT_g	T_{dec}	ΔT_{dec}
Series I				
C00S0	87.0	—	379.9	—
C00S1	91.9	—	389.2	—
C00S2	92.4	—	384.2	—
C00S3	95.2	—	386.4	—
C00S4	103.5	—	401.4	—
C00S5	107.8	—	403.5	—
Series II				
C10S0	103.6	16.6	404.2	24.3
C10S1	104.6	13.5	404.2	15.0
C10S2	105.3	12.9	412.8	28.6
C10S3	105.3	10.1	413.3	26.9
C10S4	107.1	3.6	412.1	10.7
C10S5	110.0	2.2	411.4	7.9
Series III				
C15S0	94.3	7.3	400.0	20.1
C15S1	94.4	3.3	405.6	16.4
C15S2	106.7	14.3	414.9	30.7
C15S3	106.7	11.5	414.2	27.8
C15S4	107.1	3.6	411.4	10.0
C15S5	110.0	2.2	412.8	9.3

was favorable for the dispersion in a PDMS matrix as previously described, C15A is unfavorable for the dispersion in a PS matrix compared to C10A, whose modifier has structural affinity with styrene as it has a benzyl group.[16] C15S1 has a peak of $2\theta = 2.2°$, which is similar to that in Figure 1(d) and is at a lower angle compared to C15S0, which shows that the gallery height increased from 35.3 to 40.1 Å because of the PDMS segment linked to the PS chain. The XRD pattern of C15S2 retained sharpness when compared to C10S2, although they were prepared with similar amounts of MAI. This suggests that a face–face ordered layer structure of organoclay was retained in C15S2. However, as the content of the PDMS segment was increased, this peak became obscure in the XRD patterns of C15S4 and C15S5, as shown in Figure 2 for the PS/C10A nanocomposites. These results support the fact that the PDMS segment enhanced the delamination of C15A in PS/C15A nanocomposites, similarly to the nanocomposites of 10A.

TEM

The TEM micrographs of PS/organoclay nanocomposites are displayed in Figure 4, where the dark lines represent the silicate layers in the polymer matrix.[29] Figures 4(a), 4(c), and 4(d) show that the dispersion of C10A in the polymer matrix was improved as the content of the PDMS segment was increased. In Figure 4(b), the crystallites of C10A are visible as regions of alternating narrow, dark, and light bands. It consisted of about 10–20 parallel silicate layers.[9] However, this ordered face–face layer morphology was not observable even at high magnification for C10S2, and an exfoliated structure can be observed in Figure 4(d) of C10S5. These changes in morphology by the effects of the PDMS segment linked to the PS chain were consistent with the changes of the XRD pattern shown in Figure 2. Figure 4(g) of C15S2 also shows that the dispersion of C15A was improved by the PMDS segment compared to Figure 4(e) of C15S0. Both Figure 4(f) of C15S0 and Figure 4(h) of C15S2 have ordered face–face layer structures. However, the gallery gap of C15S2 [Fig. 4(h)] was increased compared to C15S0 [Fig. 4(f)], as can be deduced from the XRD patterns of Figure 3.

Thermal properties

The T_g's of PS/organoclay nanocomposites measured by DSC are shown in Table III, where ΔT_g is the T_g difference between the sample and that in Series I prepared with a similar azo group concentration. For example, ΔT_g of C10S2 is the T_g difference between C10S2 and C00S2, and ΔT_g of C15S3 is T_g difference between C15S3 and C00S3. In Series I, the T_g was increased as the content of the PDMS segment was increased. This suggests that in these multiblock copolymers containing PDMS and PS segments, the PS segment could take more dense packing in the presence of the flexible PDMS segment. Inoue et al., also observed similar T_g increases of PMMA blocks in PDMS–PMMA multiblock copolymers prepared with MAI.[25] The fact that the T_g of C10S0 was 16.6°C higher than that of C00S0 shows that the chain mobility of PS was reduced by interaction with the silicate layers of C10A.[20] However, ΔT_g values of Series II decreased as the content of the PDMS segment in the nanocomposite was increased. This suggests that the intimate contact or interaction between the PS chain and C10A was replaced by those between the PDMS segment and C10A. In Series II, ΔT_g of C15S0 was 7.3°C, which was smaller than the ΔT_g of C10S0, 16.6°C. This shows that C15A did not disperse as well in the PS matrix as in C10A, whose modifier had benzyl group. The ΔT_g values of Series III show a first increase and then a second decrease as the content of the PDMS segment in the polymer matrix was increased. This shows that the dispersion of C15A in the polymer matrix was enhanced by the PDMS segment linked to the PS chain; however, intimate contact between the PS chain and C15A was reduced at a high PDMS segment content.

Table III also shows a 20% weight-loss temperature, T_{dec} of PS/organoclay nanocomposites measured by TGA, where ΔT_{dec} was calculated similarly to ΔT_g. For example, the ΔT_{dec} of C10S3 is a T_{dec} difference between C10S3 and C00S3. The variation of ΔT_{dec} generally showed a first increase and a second decrease as the content of PDMS segment was increased in both

Series II and III, although some exceptions existed. The first increase seemed to be attributable to the enhanced dispersion of organoclay in the polymer matrix because of the presence of the PDMS segment. The second decrease seemed to originate from a preferential distribution of organoclay into the PDMS domain at a high content of the PDMS segment content.

The results in Table III show that the differences in the thermal properties of C10S0 and C15S0 due to clay modifier can be minimized by PDMS segments. However, the thermal properties did not manifest the minute difference in the morphology of clay dispersion. For example, C10S2 and C15S2 have similar thermal properties, although the results observed by XRD and TEM indicated somewhat better dispersion of clay in C10S2 compared with C15S2.

CONCLUSIONS

The results of XRD and TEM show that the dispersion of orgnoclay in a polymer matrix was improved by the PDMS segment linked to the PS chain. However, the variations of T_g and 20% weight-loss temperature suggest that a preferential distribution of organoclay into the PDMS domain at a high PDMS segment content caused negative effects on T_g increases of the PS domains and thermal resistance of the nanocomposites.

References

1. Pinnavaia, T. J.; Beall, G. W. (Eds.) In Polymer-Clay Nanocomposites; Wiley: Chichester, 2000.
2. Giannelis, E. P. Appl Organometal Chem 1998, 12, 675.
3. Kim, B. K.; Seo, J. W.; Jeong, H. M. Eur Polym J 2003, 39, 85.
4. Ishida, H.; Campbell, S.; Blackwell, J. Chem Mater 2000, 12, 1260.
5. Zeng, C.; Lee, L. J. Macromolecules 2001, 34, 4098.
6. Huang, X.; Brittain, W. J. Macromolecules 2001, 34, 3255.
7. Okamoto, M.; Morita, S.; Taguchi, H.; Kim, Y. H.; Kotaka, T.; Tateyama, H. Polymer 2000, 41, 3887.
8. Manias, E.; Touny, A.; Wu, L.; Strawhecker, K.; Lu, B.; Chung, T. C. Chem Mater 2001, 13, 3516.
9. Vaia, R. A.; Jandt, K. D.; Kramer, E. J.; Giannelis, E. P. Chem Mater 1999, 8, 2628.
10. Vaia, R. A.; Giannelis, E. P. Macromolecules 1997, 30, 8000.
11. Gilman, J. W.; Jackson, C. L.; Morgan, A. B.; Harris, R., Jr.; Manias, E.; Giannelis, E. P.; Wuthenow, M.; Hilton, D.; Phillips, S. H. Chem Mater 2000, 12, 1866.
12. Weimer, M. W.; Chen, H.; Giannelis, E. P.; Sogah, D. Y. J Am Chem Soc 1999, 121, 1615.
13. Fan, X.; Xia, C.; Advincula, R. C. Colloids Surf A 2003, 219, 75.
14. Uthirakumar, P.; Kim, C.-J.; Nahm, K. S.; Hahn, Y. B.; Lee, Y.-S. Colloids Surf A 2004, 247, 69.
15. Uthirakumar, P.; Nahm, K. S.; Han, Y. B.; Lee, Y.–S. Eur Polym J 2004, 40, 2437.
16. Doh, J. G.; Cho, I. Polym Bull 1998, 41, 511.
17. Yoon, J. T.; Jo, W. H.; Lee, M. S.; Ko, M. B. Polymer 2001, 42, 329.
18. Lim, Y. T.; Park O. O. Rheol Acta 2001, 40, 220.
19. Akelah, A.; Moet, A. J Mater Sci 1996, 31, 3589.
20. Laus, M.; Camerani, M.; Lelli, M.; Sparnacci, K.; Sandrolini, F.; Francescangeli, O. J Mater Sci 1998, 33, 2883.
21. Burnside, S. D.; Giannelis, E. P. Chem Mater 1995, 7, 1597.
22. Liao, B.; Song, M.; Liang, H.; Pang, Y. Polymer 2001, 42, 10007.
23. Fischer, H. R.; Gielgens, L. H.; Koster, T. P. M. Acta Polym 1999, 50, 122.
24. Inoue, H.; Ueda, A.; Nagai, S. J Polym Sci Part A: Polym Chem 1988, 26, 1077.
25. Inoue, H.; Ueda, A.; Nagai, S. J Appl Polym Sci 1998, 35, 2039.
26. Nakamura, K.; Fujimoto, K.; Kawaguchi, H. Colloids Surf A 1999, 153, 195.
27. Bera, P.; Saha, S. K. Indian J Chem Technol 1999, 6, 24.
28. Le Baron, P. C.; Wang, Z.; Pinnavaia, T. J Appl Clay Sci 1999, 15, 11.
29. Hoffmann, B.; Dietrich, C.; Thomann, R.; Friedrich, C.; Mülhaupt, F. Macromol Rapid Commun 2000, 21, 57.